0026-895X/97/030362-11$3.00/0

MOLECULAR PHARMACOLOGY, **52:**362–372 (1997).

Developmentally Regulated Expression of the *CYP4A* Genes in the Spontaneously Hypertensive Rat Kidney

DEANNA L. KROETZ, LINN M. HUSE, ANNELI THURESSON, and MARK P. GRILLO

Departments of Biopharmaceutical Sciences (D.L.K., L.M.H., A.T., M.P.G.) and Pharmaceutical Chemistry (D.L.K.), School of Pharmacy, and the Liver Center, School of Medicine (D.L.K.), University of California San Francisco, San Francisco, California 94122

Received February 20, 1997; Accepted May 12, 1997

SUMMARY

The CYP4A enzymes catalyze the formation of 20-hydroxyeicosatetraenoic acid (20-HETE), which has potent effects on the renal vasculature and tubular ion transport. Based on an increased 20-HETE formation in renal microsomes from spontaneously hypertensive rats, it has been proposed that increased expression of the *CYP4A* genes is an early event in the development of hypertension in these animals. To test this hypothesis, we developed RNase protection assays for specific detection of the individual *CYP4A* genes in the kidneys of spontaneously hypertensive and Wistar-Kyoto rats. Distinct age-dependent patterns of expression were observed for the individual *CYP4A* genes, with only CYP4A3 mRNA measurable in the kidneys of 1-week-old rats. CYP4A1 and CYP4A8 mRNA were detectable by 3 weeks of age and CYP4A2 mRNA at 5 weeks of age. The expression of CYP4A1 and CYP4A3 varied 4–5-fold throughout development and was highest between 3 and 5 weeks of age, declining steadily thereafter to 20% of their maximal level by 9 weeks of age. CYP4A2 mRNA levels increased steadily between 5 and 9 weeks of age, whereas CYP4A8 mRNA levels were relatively constant throughout development. The CYP4A3 mRNA level was significantly increased 1.6–2-fold in the cortex and outer medulla of 1–4-week-old spontaneously hypertensive rat kidneys relative to the corresponding level in the Wistar-Kyoto. A similar 1.4–1.7-fold increase in CYP4A8 mRNA was also found in 3- and 4-week-old spontaneously hypertensive kidneys. Accompanying the increased expression of CYP4A3 and CYP4A8 mRNA in the prehypertensive rats were corresponding changes in functional CYP4A measured as either arachidonic acid or lauric acid ω-hydroxylase activity (1.4–2.0-fold increases) and CYP4A protein levels. After 4 weeks of age, the level of CYP4A mRNA, enzyme activity, and protein were similar in the kidneys of Wistar-Kyoto and spontaneously hypertensive rats. The findings suggest that the expression of CYP4A3 and CYP4A8 may be critical to the early changes in eicosanoid formation and renal function in the young spontaneously hypertensive rat.

In addition to their role in the metabolism of xenobiotics, the CYP enzymes play an important role in the biotransformation of a number of endogenous compounds, including fatty acids, prostaglandins, vitamins, bile acids, and steroids (1). Cytochrome P450-mediated metabolism of arachidonic acid leads to the formation of a number of distinct eicosanoids with potent effects on renal tubular ion transport and vascular tone. The ω-hydroxylated product, 20-HETE, inhibits Na^+/K^+-ATPase and the 70-pS K^+ channel in the medullary thick ascending limb (2, 3), is involved in tubuloglomerular feedback and the autoregulation of renal blood flow and glomerular filtration rate (4), and causes dose-dependent vasoconstriction of renal arcuate arteries (5). In contrast, the ω-1 hydroxylated metabolite, 19-HETE, stimulates Na^+/K^+-ATPase and dilates renal arteries in a stereospecific fashion (5, 6). EETs and their corresponding dihydroxy derivatives (DHETs) also have vasoactive properties and can modulate intracellular ion concentrations throughout the nephron (7, 8). Thus, CYP-catalyzed arachidonic acid metabolism is important in the regulation of renal function and vascular tone.

In the SHR, a well-established experimental model for human essential hypertension, renal transplantation studies support a role for renal dysfunction in the development of hypertension (9). Renal functional disturbances are evident in the SHR before the development of hypertension and are essential for the development and maintenance of the elevated blood pressure (10). A growing body of evidence has led to the proposal that modulation of CYP-catalyzed eicosanoid formation is an important mediator of the changes in renal function and accompanying alterations in blood pressure in the SHR (11, 12). Alterations in arachidonic acid metabolism

This work was supported in part by a New Investigator Award from the American Association of Colleges of Pharmacy, a Research Starter Grant from the Pharmaceutical Research and Manufacturers Association, the University of California San Francisco Academic Senate, and National Institutes of Health Grant HL53994.

ABBREVIATIONS: HETE, hydroxyeicosatetraenoic acid, EET, epoxyeicosatrienoic acid; DHET, dihydroxyeicosatrienoic acid; SHR, spontaneously hypertensive rat; WKY, Wistar-Kyoto; RT-PCR, reverse transcription-polymerase chain reaction; GAPDH, glyceraldehyde 3-phosphate dehydrogenase; HPLC, high performance liquid chromatography; GC-MS, gas chromatography-mass spectrometry; nt, nucleotide(s); bp, base pair(s).

in the SHR kidney are specific for the ω- and ω-1-hydroxylation pathways. Increased formation of 20-HETE has been reported in renal microsomes from SHR rats relative to the WKY normotensive strain, with the most significant increases occurring in young prehypertensive rats (13–16). At 4 weeks of age, increased production of 20-HETE in the cortex of the SHR was accompanied by decreased diameter of interlobular arteries and afferent arterioles (15). However, despite augmented differences in the internal diameter of these vessels in 9–12-week-old SHR animals, increased 20-HETE formation in the SHR kidney was no longer apparent (12). Similar increases in 19-HETE formation in renal microsomes from SHR rats have been described through 9 weeks of age (13). The administration of heme oxygenase inducers to indirectly inhibit renal cytochrome P450 enzymes has provided *in vivo* evidence for a role for 20-HETE in the regulation of blood pressure. Treatment with $SnCl_2$ reduced blood pressure in 7-week-old SHR rats to normotensive levels and inhibited 20-HETE formation in renal microsomes (11). Furthermore, urinary concentrations of 20-HETE were significantly increased in 7-week-old SHR rats relative to WKY animals (17).

Purified or expressed forms of each of the rat CYP4A enzymes metabolize arachidonic acid and other fatty acids at the ω and ω-1 positions, with a clear preference for the terminal position (18, 19). However, the *in vivo* contribution of the individual CYP4A isoforms to the metabolism of arachidonic acid and other fatty acids has not yet been characterized. The CYP4A enzymes seem to be entirely responsible for the ω-hydroxylase activity, whereas both CYP2C and CYP2E isoforms also contribute to fatty acid ω-1-hydroxylase activity (20, 21). The wide distribution of arachidonic acid ω-1-hydroxylase activity throughout the nephron is consistent with multiple enzyme involvement in this reaction (14). In the rat kidney, four *CYP4A* genes are expressed: *CYP4A1*, *CYP4A2*, *CYP4A3*, and *CYP4A8*. The nucleotide and amino acid similarity of these genes ranges from 62% to 97% (22, 23). Evidence supporting altered expression of one of the CYP4A proteins or genes in the SHR kidney is limited. Increased CYP4A2-immunoreactive protein and ω- and ω-1-hydroxylation of lauric acid was reported in the kidneys of 12-week-old SHR rats relative to WKY animals (24). These changes in CYP expression seem to be specific because the renal content of CYP2C23 and CYP4A8 was unaltered in the hypertensive animals. The level of CYP4A2 mRNA in 4-week-old SHR rats was reported to be four times the level in age-matched WKY rats, although expression was similar in adult rats (25).

Attempts to identify the specific CYP4A proteins responsible for the increased formation of 20-HETE in the young SHR have been limited by the lack of specific probes for the multiple genes and their corresponding proteins. To characterize CYP4A expression and regulation in the rat kidney, we developed gene-specific RNase protection assays for the CYP4A mRNAs. Using this assay, the expression of the renal *CYP4A* genes was characterized throughout development, and differences in expression between prehypertensive SHR and WKY rats were detected. Coordinate changes in CYP4A mRNA, protein, and activity levels suggest that increased CYP4A expression is an important contributor to the renal function disturbances during this critical period of development. The distinct age-dependent pattern of expression of the individual *CYP4A* genes is consistent with diverse roles for these proteins in the maintenance of renal function and blood pressure during development.

Experimental Procedures

Materials. Radiolabeled nucleotides, arachidonic acid, and lauric acid were purchased from Amersham (Arlington Heights, IL). Restriction enzymes were obtained from New England Biolabs (Beverly, MA), and modifying enzymes were from GIBCO BRL (Gaithersburg, MD). All molecular biology grade chemicals, HPLC solvents, and ScintiVerse LC were from Fisher Scientific (Pittsburgh, PA). Arachidonic acid and lauric acid were purchased from Nu Chek Prep (Elysian, MN) and 20-HETE and 12-hydroxylauric acid were from Sigma Chemical (St. Louis, MO). Dihydroxyeicosatrienoic acid standards were from Oxford Biomedical Research (Oxford, MI). Oligonucleotides were synthesized by the Biomolecular Resource Center at the University of California, San Francisco. Nitrocellulose membranes were from Micron Separations (Westborough, MA), and the anti-rat CYP4A1 antisera from Daiichi Pure Chemicals was distributed by Genetest (Woburn, MA). All other reagents were of the highest grade available and were purchased from Fisher Scientific or Sigma Chemical.

CYP4A plasmid constructs. A full-length CYP4A1 cDNA in pBR322 and a full-length CYP4A3 cDNA in pUC9 were kindly provided by Dr. Frank J. Gonzalez (National Cancer Institute, Bethesda, MD). Both cDNAs were excised from their original plasmids by digestion with *Eco*RI and were ligated into pGEM-7Zf(+) (Promega, Madison, WI). The CYP4A1 riboprobe construct was made by inserting the 1191-bp *Acc*I/*Sac*I fragment from the full-length construct into pGEM-4Z (Promega). For the CYP4A3 riboprobe construct, a 312-bp *Eco*RI/*Hin*dIII fragment was isolated from the full-length cDNA and ligated into pGEM-7Zf(+). A 212-bp CYP4A2 cDNA fragment for use as a riboprobe was isolated from rat kidney RNA through RT-PCR using the following primers based on the published genomic sequence of CYP4A2 (22): forward, 5′-GGAATTC-CCAAAGCCTTATCAATCC-3′; and reverse, 5′-TCTCTAGAGGGT-GATCCTGG-3′. The forward primer spanned a 9-nt deletion between CYP4A2 and CYP4A3 to ensure that only the former cDNA was amplified, and the underlined nucleotides represent an *Eco*RI restriction site that was added to the primer. An *Xba*I restriction site (underlined) was present in the region spanning the reverse primer. Total kidney RNA was reverse-transcribed using a poly(dT) primer and Moloney murine leukemia virus reverse transcriptase. The reaction product was subsequently amplified by 30 cycles of PCR using the indicated primers and *Taq* DNA polymerase (Perkin-Elmer Cetus, Norwalk, CT) with the following conditions: 94° for 1 min, 55° for 1 min, and 72° for 30 sec, followed by a single final extension for 15 min at 72°. The amplified fragment of expected size was digested with *Eco*RI and *Xba*I and ligated into pGEM-11Zf(+) (Promega). A full-length CYP4A2 cDNA (1673-bp) was isolated by RT-PCR using a similar strategy and the following primers: forward, 5′-GGGGTAC-CCCAGACCCTAGTGATCCAGA-3′; and reverse, 5′-CCATCGATG-GCAGAAGGATGGGAATCAAAG-3′. The underlined nucleotides indicate restriction sites for *Kpn*I and *Cla*I, respectively, that were present in the primer regions and used for ligation of the PCR product into pGEM-7Zf(+). A 398-bp CYP4A8 cDNA fragment for use as a riboprobe (forward primer, 5′-CACAGTCATGCTCTCCTTC-3′; and reverse primer, 5′-GAGATGTGAGCAGATGGAGTG-3′) and a full-length 1712-bp cDNA (forward primer, 5′-CCATCGATG-GCATGAGTGGCTCT-3′; and reverse primer, 5′-GCTCTAGAAAA-GACTGACAGACAAGG-3′, with *Cla*I and *Xba*I restriction sites, respectively) were also isolated by RT-PCR. Primers for the CYP4A8 cDNA were based on published sequence (23). The full-length CYP4A8 cDNA was ligated directly into pT7Blue(R) (Novagen, Madison, WI), and the partial CYP4A8 fragment was ligated into pGEM-7Zf(+) using internal *Cla*I and *Sph*I restriction sites. The identities

of all of the constructs generated by RT-PCR were confirmed by DNA sequencing of the entire inserts using dideoxy-mediated chain termination and Sequenase 2.0 (United States Biochemical, Cleveland, OH). The first 249 bp of the rat GAPDH cDNA was isolated from a full-length cDNA and ligated into pT7Blue(R) as a control riboprobe.

Animals and tissue collection. Male WKY rats and SHR were purchased from Charles River Laboratories (Wilmington, MA) and maintained in a controlled housing environment with 12-hr light/dark cycles and fed standard laboratory chow for ≥3 days before they were killed. All animal use was approved by the University of California San Francisco Committee on Animal Research and followed the National Institutes of Health guidelines for the care and use of experimental animals. Rats were anesthetized with ether, the abdominal cavities were opened, and the kidneys were perfused with ice-cold saline. Perfused kidneys were rapidly removed and either frozen immediately in liquid nitrogen or dissected into cortex, outer medulla, and inner medulla before immersion in liquid nitrogen. Frozen tissue was stored at −80° until preparation of RNA or microsomes.

Ribonuclease protection assays. Total RNA was isolated from whole kidneys by homogenization in guanidinium thiocyanate and equilibrium centrifugation through a cesium chloride gradient and from dissected kidneys by acid-phenol extraction (26). Ribonuclease protection assays were performed essentially as described by Hod (27). The riboprobe constructs were linearized with appropriate restriction enzymes such that the protected fragments spanned the following regions of the cDNA sequence: 1285–1557 nt of CYP4A1, 343–549 nt of CYP4A2, 214–526 nt of CYP4A3, 1300–1563 nt of CYP4A8, and 2–250 nt of GAPDH. CYP4A and GAPDH riboprobes were radiolabeled with [α-^{32}P]CTP and gel-purified on a 6% polyacrylamide/8 M urea gel. Labeled probes were eluted from the gel with a solution of 0.5 M ammonium acetate, 0.2% sodium dodecyl sulfate, and 1 mM EDTA. Total kidney RNA (5–10 μg) was simultaneously hybridized with one of the CYP4A probes and the GAPDH probe in 20 μl of a buffer containing 80% formamide, 20 mM sodium citrate, pH 6.4, 60 mM sodium acetate, pH 6.4, and 0.2 mM EDTA. The sample-probe mixture was denatured at 90° for 5 min and hybridized overnight at 42°. The RNA-probe hybrids were then digested with a 1:200 dilution of RNase A/T_1 cocktail (Ambion, Austin, TX) in a buffer of 100 mM Tris·HCl, pH 7.5, 5 mM EDTA, and 200 mM sodium acetate for 1 hr at 30°. An equal volume of a solution of 4 M guanidinium thiocyanate, 100 mM Tris·HCl, pH 7.4, 100 μg/ml tRNA, 0.5% sarkosyl, and 1% β-mercaptoethanol was added to inactivate the ribonucleases, and RNA was precipitated with isopropanol. RNA pellets were air-dried and resuspended in 80% formamide, 2 mM EDTA, pH 8.0, 0.1% bromphenol blue, and 0.1% xylene cyanol for separation of protected fragments on a 5% denaturing polyacrylamide gel. After electrophoresis, the gel was transferred to blotting paper, vacuum dried, and exposed to X-ray film at −80° with an intensifying screen. Autoradiographs were scanned with a laser densitometer (Ultro Scan XL; Pharmacia LKB, Piscataway, NJ), and the level of a given CYP4A mRNA was expressed relative to the level of GAPDH.

RT-PCR of CYP4A2 and CYP4A3. CYP4A2 mRNA was detected in the kidneys of 1–13-week-old WKY rats and SHR by RT-PCR of a 212-bp fragment as described above. The following primer was designed to detect both CYP4A2 and CYP4A3 simultaneously: 5′-ACAACCTGAAGGACAGAG-3′; it was paired with the reverse CYP4A2 primer described above to amplify a 350-bp (CYP4A2) or 359-bp (CYP4A3) fragment from the same samples. The deletion of an *Apo*I restriction site in this region of the CYP4A2 cDNA was used to distinguish between CYP4A2 and CYP4A3 in these amplified samples. Amplified DNA fragments were separated on a 2% agarose gel and visualized by ethidium bromide staining.

Renal fatty acid metabolism. Renal microsomes were prepared from frozen kidney tissue as previously described (24) and stored at −80°. An ethanolic solution of sodium arachidonate (containing 0.2 μCi [1-^{14}C]arachidonic acid) was evaporated and resuspended in a 0.5-ml reaction mix containing 0.25 mg of microsomal protein, 50 mM Tris·HCl, pH 7.4, 150 mM KCl, 10 mM $MgCl_2$, 8 mM sodium isocitrate, and 0.5 IU isocitrate dehydrogenase. The final concentration of arachidonic acid was 0.01 mM. After incubation at 37° for 3 min in a shaking water bath in an atmosphere of air, the reaction was initiated by the addition of NADPH to a final concentration of 1 mM. The reactions were stopped after 30 min by the addition of 0.5 N HCl to a final pH of 3–3.5. Arachidonic acid and its metabolites were extracted from the aqueous mixture twice with 2 ml of ethyl acetate. The ethyl acetate phases were combined and washed with water before evaporation under nitrogen. The metabolism of lauric acid was measured in a similar fashion as described for arachidonic acid except that the protein concentration was 0.25 mg/ml, lauric acid concentration was 0.1 mM (0.1 μCi of [1-^{14}C]lauric acid), and the reaction was terminated after 5 min. Lauric acid and its metabolites were extracted with 2.5 ml of diethyl ether and the organic phase evaporated under nitrogen. In both cases, extracted samples were stored at −80° under nitrogen until analysis by HPLC. Reverse-phase HPLC with radiometric detection was used to separate and quantify arachidonic acid and lauric acid metabolites. The HPLC system consisted of a Shimadzu (Kyoto, Japan) SLC-6A controller and two LC-6A pumps with a gradient mixer coupled with a Radiomatic 525TR Flow Scintillation Analyzer and Flo-One software (Packard, Downers, IL). Metabolites were separated on a 250 × 4.6-mm Alltima C18 5-μm column with an Alltima C18 guard column and in-line filter (Alltech Associates, Deerfield, IL) using conditions previously described (28).

GC-MS analysis of arachidonic acid metabolites. Microsomal incubations with arachidonic acid and metabolite separation by reverse-phase HPLC were performed as described above. Fractions were collected every 0.5 min, and those containing the major metabolites were identified by liquid scintillation counting. Acetonitrile was removed from the pooled metabolite fractions *in vacuo*, and the acidified aqueous phase was extracted three times with ethyl acetate. The combined ethyl acetate phases were dried with magnesium sulfate and evaporated to dryness under a stream of nitrogen gas. The methyl ester derivatives were prepared by the addition of an ethereal solution of diazomethane (200 μl) for 10 min at room temperature. The trimethylsilyl ether derivatives were then prepared by incubation of the extract with 100 μl of bis(trimethylsilyl)trimethylfluoroacetamide for 30 min at 100°. GC-MS was carried out on a Hewlett-Packard instrument (model 5710A; Hewlett-Packard, Avondale, PA) that was interfaced directly to the ion source of a VG 70–70H double-focusing magnetic sector mass spectrometer. Metabolites were separated on a fused silica capillary GC column (30 m × 0.32-mm i.d., 0.25-μm film thickness) coated with DB-1 bonded stationary phase (J&W Scientific, Rancho Cordova, CA), with helium used as the carrier gas (head pressure, 20 lbs/sq. inch). The column oven temperature was programmed linearly from 80° to 180° at 20°/min and then from 180° to 290° at 10°/min. Mass spectrometry was performed in the total ion monitoring mode, and analyses were performed in the EI mode with an electron energy of 70 eV, a trap current of 200 μA, and an accelerating potential of 4 kV.

Immunoblotting of CYP4A proteins. Renal microsomes (10 μg) were subjected to sodium dodecyl sulfate-polyacrylamide gel electrophoresis followed by Western immunoblotting using goat polyclonal antibodies against rat liver CYP4A1 (26). Microsomal proteins were separated on a 8% polyacrylamide gel at 10 mA and transferred to nitrocellulose in 25 mM Tris/192 mM glycine/20% methanol using a semidry transfer system (BioRad, Hercules, CA). Western blots were incubated with a 500-fold dilution of goat anti-CYP4A1 serum followed by a 1000-fold dilution of alkaline phosphatase-conjugated rabbit anti-goat IgG. Immunoreactive proteins were detected using an alkaline phosphatase conjugate substrate kit (BioRad).

Statistics. All measurements were performed on RNA or protein samples from individual rats, and results are expressed as mean ± standard deviation for three to six animals of a given age and strain. Statistical significance of differences between mean values was eval-

uated by an unpaired Student t test. A value of $p < 0.05$ was considered to be statistically significant.

Results

Renal CYP4A expression. A specific RNase protection assay was developed to detect CYP4A1, CYP4A2, CYP4A3, and CYP4A8 mRNA expressed in the rat kidney. The specificity of each of the CYP4A riboprobes was confirmed with hybridizations of the probes with RNA transcribed *in vitro* from the full-length cDNA of each *CYP4A* gene (Fig. 1). The CYP4A1 riboprobe detected a 272-nt protected fragment when hybridized with either the full-length CYP4A1 sense RNA or total RNA from a WKY rat kidney. Likewise, the CYP4A8 riboprobe detected a 263-nt protected fragment in kidney RNA samples that was identical to the corresponding hybridization with CYP4A8 sense RNA. The CYP4A2 and CYP4A3 mRNA sequences are 97% identical and include a 9-bp deletion in the *CYP4A2* gene (22). The CYP4A3 riboprobe spanned this deletion and made it possible to detect both a 312-nt CYP4A3 protected fragment and a 170-nt protected CYP4A2 fragment with this single probe. The corresponding 133-nt CYP4A2 fragment was subject to further RNase digestion at several single base mismatches and was generally not detected. All measurements of CYP4A2 mRNA levels were therefore based on the 170-nt protected fragment from hybridization with the CYP4A3 probe. Due to the very high degree of homology, cross-hybridization of each of the CYP4A probes with the related CYP4A mRNAs was evident; however, these imperfect hybrids resulted in smaller protected fragments that did not interfere with the detection of the fragment of interest. All protected fragments from hybridization of rat kidney RNA with a given CYP4A riboprobe could be attributed to a known CYP4A mRNA, suggesting that additional members of this gene family are not likely to be expressed in rat kidney. Ribonuclease protection assays were carried out using conditions of probe excess so quantification of the CYP4A mRNA levels was possible. Preliminary experiments established the linearity of these assay conditions with up to 20 μg of sample RNA.

Distinct developmental patterns of expression were detected for the individual *CYP4A* genes, as illustrated in Fig. 2. Expression of the CYP4A/GAPDH mRNA ratios at each age relative to the ratio in mature 13-week-old WKY rats illustrates the age- and strain-dependent differences in expression of each of the *CYP4A* genes. The expression of GAPDH showed no evidence of either strain- or age-related differences and was therefore considered an appropriate control gene. Only CYP4A3 mRNA was detectable in kidneys of 1-week-old WKY rats and SHR, although levels were one fourth to one half of the level in mature WKY rats. By 3 weeks of age, both CYP4A1 and CYP4A8 mRNAs could also be detected although the level of CYP4A1 was too low and variable to be accurately quantified. The expression of CYP4A8 was tightly regulated by changes associated with weaning because it could not be detected in 3-week-old weanling rats but was expressed at levels comparable to or greater than those observed in mature rats in RNA prepared from weaned 3-week-old rats (data not shown). CYP4A2 expres-

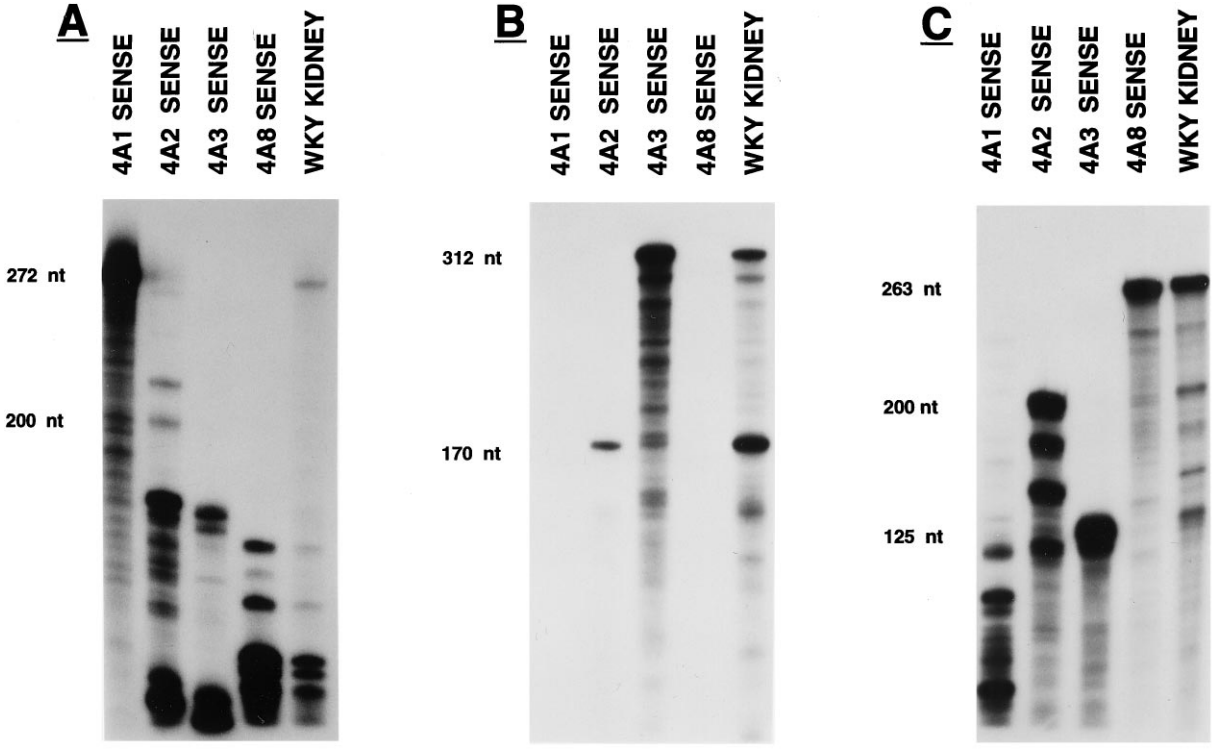

Fig. 1. Specificity of CYP4A ribonuclease protection assay. The CYP4A1 (A), CYP4A3 (B), and CYP4A8 (C) riboprobes were hybridized with a full-length CYP4A sense RNA transcribed *in vitro* from the corresponding cDNA (10 pg) or total kidney RNA (5 μg) prepared from a 9-week-old WKY rat. The major 272-nt CYP4A1 and 263-nt CYP4A8 protected fragments detected in the kidney sample were as expected from hybridization with the corresponding sense RNA control. The CYP4A3 probe detects both a 312-nt protected CYP4A3 fragment and a 170-nt protected CYP4A2 fragment as predicted from the sense hybridizations. The additional smaller fragments in the kidney samples were consistent with cross-hybridization of the probes with related members of the CYP4A family.

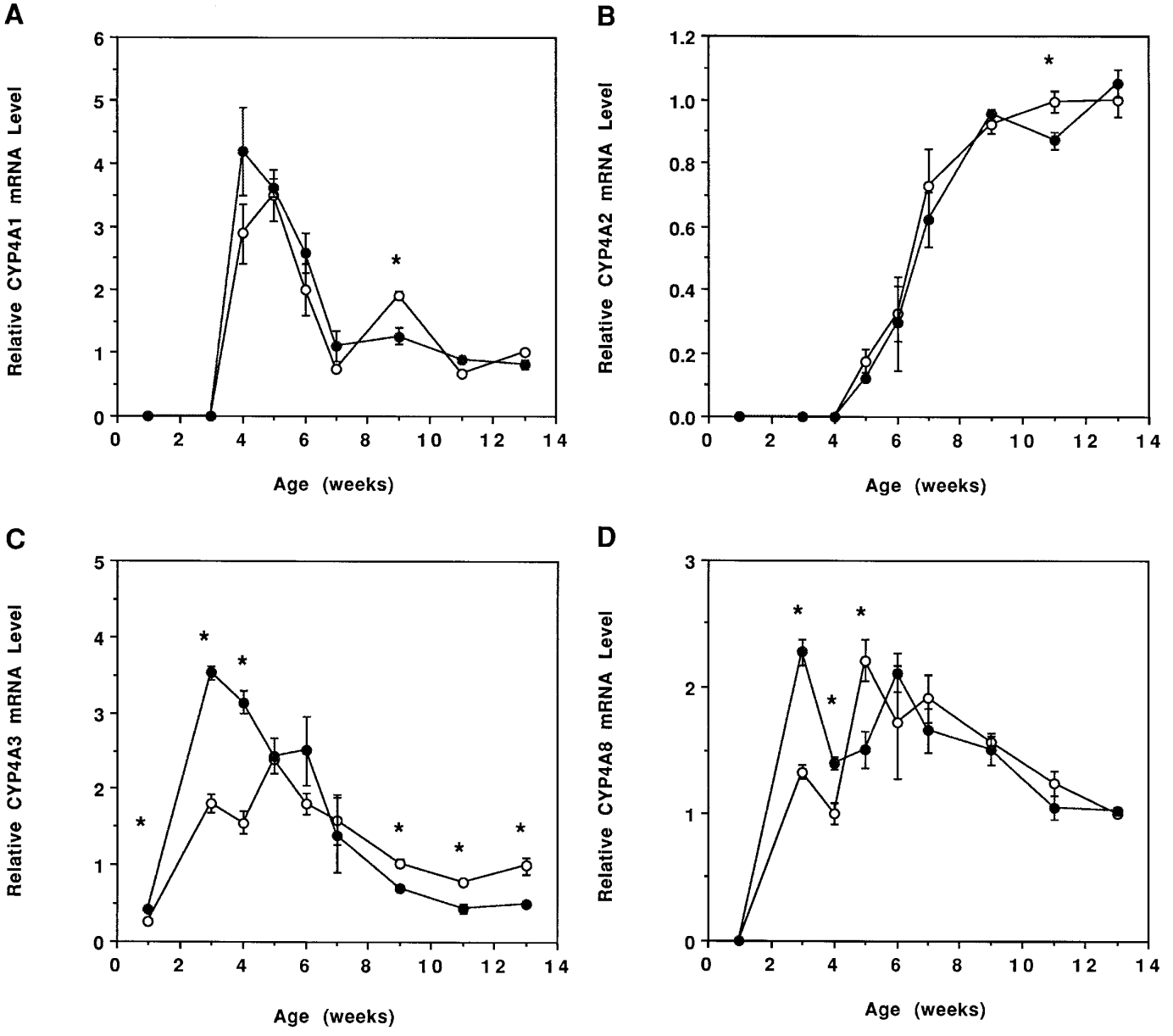

Fig. 2. Relative levels of CYP4A mRNA in WKY rat and SHR kidneys. Renal CYP4A1 (A), CYP4A2 (B), CYP4A3 (C), and CYP4A8 (D) mRNA levels were measured in samples from WKY rat (○) and SHR (●) by RNase protection assay and quantified by laser densitometry. The CYP4A/GAPDH mRNA ratio for a given age and strain is expressed relative to that in the 13-week-old WKY rat sample to illustrate both age-dependent changes and strain differences in expression. Values are mean ± standard deviation from three to six animals of a given age and strain. Significant differences between WKY rat and SHR kidneys at a given age are indicated ($p < 0.05$).

sion was not detectable by RNase protection assay until 5 weeks of age and steadily increased until 9 weeks. Expression of CYP4A1 and CYP4A3 mRNA showed a large variation between young and mature rats (4–5-fold), and for both of these genes, expression was maximal between 3 and 5 weeks of age and declined steadily after this time, coincident with the detectable expression of the *CYP4A2* gene. In contrast, after 3 weeks, CYP4A8 mRNA levels were fairly constant throughout development. Expression of all of the *CYP4A* genes was relatively constant after 9 weeks of age.

Significant differences in CYP4A3 expression between hypertensive and normotensive rats were found in both young and mature animals (Fig. 2C). CYP4A3 was increased 1.6–2-fold in the kidneys of 1–4-week-old SHR relative to age-matched WKY rats, whereas the level of CYP4A3 expression in 9–13-week-old SHR kidneys was only 50–70% of the corresponding level in WKY rat kidneys. Kidney dissection indicated that the differences in CYP4A3 expression between WKY rats and SHR are similar in the cortex and outer medulla (data not shown). The only other notable interstrain difference in CYP4A expression was a 1.4–1.7-fold increase in CYP4A8 expression in 3- and 4-week-old SHR (Fig. 2D), which was variable among separately purchased groups of rats. Surprisingly, mRNA levels were similar in the cortex and outer medulla for all of the *CYP4A* genes, with the exception of CYP4A1 (data not shown). In this case, expression in the outer medulla was consistently 50−80% of that in the cortex. No additional differences between WKY rats and SHR were detected on analysis of RNA from dissected kidneys, and interstrain comparisons made with whole and dis-

sected kidney were identical for each of the genes. There was no detectable expression of any of the *CYP4A* genes in the inner medulla.

CYP4A2 mRNA levels were previously reported to be increased several-fold in the kidneys of 4-week-old SHR relative to WKY rats (25). Therefore, we used an RT-PCR approach to confirm the lack of CYP4A2 expression in immature kidneys. Using CYP4A2-specific primers, barely detectable levels of CYP4A2 expression were evident in kidneys of 1–4-week-old WKY rats and SHR (Fig. 3A). Expression increased dramatically between 4 and 5 weeks of age, which was the point at which CYP4A2 mRNA was detectable by RNase protection assay (Fig. 2B). Consistent with measurable expression of CYP4A3 by RNase protection assay as early as 1 week of age, an expected fragment could be amplified from 1–13-week-old kidneys using primers that would anneal to both CYP4A3 and CYP4A2 cDNAs (Fig. 3B). An *Apo*I restriction site that was deleted in this region of the CYP4A2 cDNA was used to distinguish between CYP4A2 and CYP4A3 in the 360-bp fragment amplified with the nonspecific primers. Both CYP4A2 and CYP4A3 have *Apo*I restriction sites at positions 18 bp and 48 bp in the amplified fragment, whereas CYP4A3 has an additional *Apo*I site at 159 bp. In the 1- and 3-week-old samples, only the 101- and 201-bp restriction fragments consistent with the *Apo*I sites in the CYP4A3 cDNA were detected, whereas in the 4- and 5-week-old samples, both the 303-bp fragment corresponding to CYP4A2 and the two smaller fragments corresponding to CYP4A3 were detected (Fig. 3C). Consistent with the high level of expression of CYP4A2 relative to CYP4A3 in the 7- and 13-week-old kidneys, only the CYP4A2 fragment was evident in the amplification products from these samples.

Renal arachidonic acid metabolism. As expected on the basis of previous investigations (13, 15), multiple metabolites were produced from incubation of rat renal microsomes with arachidonic acid (Fig. 4). All detectable metabolites were NADPH dependent (data not shown). Optimal chromatographic separation permitted individual quantification of the 14,15-, 11,12-, and 8,9-regioisomeric DHETs and 19- and 20-HETE. For the purposes of this study, the individual EET regioisomers and stereoisomers were not identified, and the EET formation rate was calculated from the sum of all

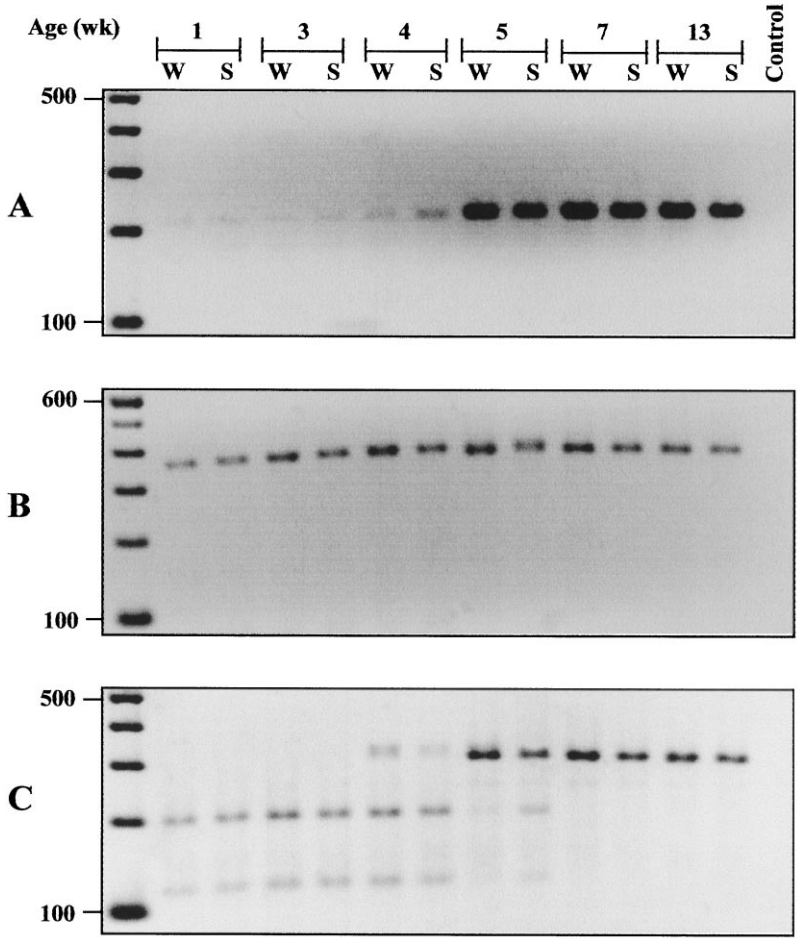

Fig. 3. RT-PCR of CYP4A2 and CYP4A3 in the WKY rat and SHR kidneys. Renal RNA from 1–13-week-old WKY rat (*W*) and SHR (*S*) was reverse-transcribed and amplified by PCR with either CYP4A2-specific primers (A) or primers that anneal to both CYP4A2 and CYP4A3 (B). Both primer pairs amplified a single product of expected size, and no DNA was detected in control samples in which the RNA was omitted in the reverse-transcription reaction. The amplified fragments were separated on a 2% agarose gel with a 100-bp molecular weight ladder, and a representative inverse image of an ethidium bromide-stained gel is shown. The DNA fragments in B were digested with *Apo*I (C) to distinguish between CYP4A3 cDNA (101- and 201-bp restriction fragments) and CYP4A2 cDNA (303-bp restriction fragment). CYP4A3 expression is measurable throughout the 1–13-week period of development, whereas only very low levels of CYP4A2 mRNA were detectable before 5 weeks of age.

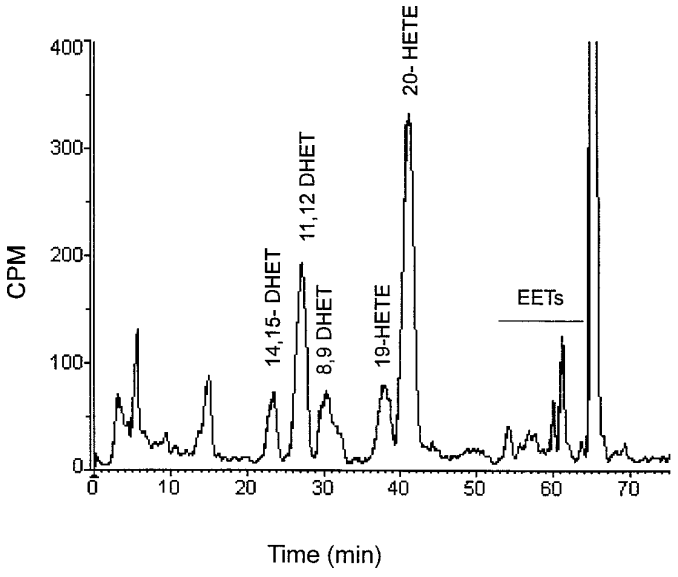

Fig. 4. Representative chromatogram (from HPLC) illustrating the separation and radiometric detection of NADPH-dependent metabolites of arachidonic acid formed in rat renal microsomes. Renal cortical microsomes from a 7-week-old SHR were incubated with [^{14}C]arachidonic acid, and the metabolites were extracted as described in the text. The DHET and HETE metabolites were identified by GC-MS, and EETs were calculated as all radiolabeled metabolites eluting between 50 and 63 min. Arachidonic acid elutes at 67 min.

metabolites eluting between 50 and 63 min. Epoxygenase activities are expressed as the sum of EET and DHET formation. The structural identity of the DHET and HETE metabolites was confirmed by GC-MS analysis. All metabolite spectra were in agreement with published results (29, 30) and the corresponding spectra of commercially available DHET and 20-HETE standards. All reactions were performed under conditions that were linear with respect to protein and time. The substrate concentration used in these studies (10 μM) was much lower than the estimated K_m value for 20-HETE formation with rat renal microsomes (134 ± 28 μM).

Total renal metabolism of arachidonic acid increased >2-fold between 3 and 13 weeks of age, and there were no qualitative differences in metabolism between WKY and SHR rat kidneys. Formation of 20-HETE in 1-week-old kidneys was evident, although it was close to the limit of detection. In SHR and WKY rats ≤6 weeks of age, epoxygenase activity accounted for 50–70% of total arachidonic acid metabolism. However, in older rats, 20-HETE was the major renal metabolite (50–64% of total metabolism). Because our analysis did not detect further metabolism of 20-HETE to the dicarboxylic acid metabolite, arachidonic acid ω-hydroxylation should be an accurate measure of CYP4A activity. The contribution of the ω-1-hydroxylation pathway to overall arachidonic acid metabolism was fairly constant throughout development and ranged from 2% to 8%.

CYP4A enzyme activity, as reflected by arachidonic acid ω-hydroxylation, increased between 3 and 9 weeks of age and then remained fairly constant through 13 weeks of age (Fig. 5A). The formation of 20-HETE increased almost 5-fold between 3- and 9-week-old SHR and WKY rats (e.g., from 7.68 ± 0.92 pmol/min/mg of protein in 3-week-old SHR kidneys to 36.0 ± 4.74 pmol/min/mg of protein in 9-week-old

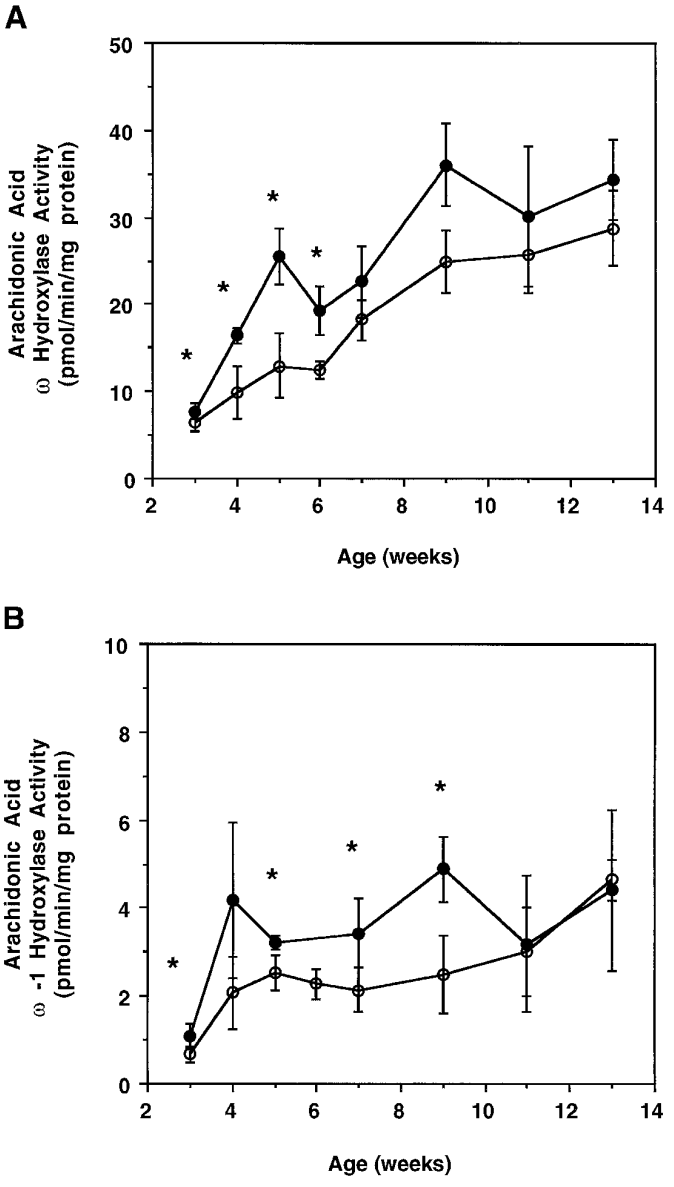

Fig. 5. Renal arachidonic acid ω- and ω-1-hydroxylase activity throughout development in the WKY rat and SHR. Arachidonic acid ω- (A) and ω-1- (B) hydroxylase activity was measured as the NADPH-dependent formation of 20-HETE and 19-HETE, respectively, in incubations of WKY rat (○) and SHR (●) renal microsomes with [^{14}C]arachidonic acid. Values are mean ± standard deviation from three to six animals of a given age and strain. Significant differences between WKY rat and SHR kidneys at a given age are indicated ($p < 0.05$). Arachidonic acid ω-hydroxylase activity reflects CYP4A enzyme activity, whereas 19-HETE formation is also dependent on CYP2C and CYP2E1 activity.

SHR kidneys). Although there was a trend toward increased 20-HETE formation in SHR compared with WKY rats at all ages, these differences reached statistical significance only in the 3–6-week-old animals. The largest differences were found in 4- and 5-week-old SHR rats (1.7- and 2.0-fold increase over the corresponding WKY samples, respectively). The ratio of 19-HETE to 20-HETE formation ranged from 1:5 to 1:10 and was similar for the hypertensive and normotensive rats. The formation of 19-HETE showed a similar developmental pattern as 20-HETE and increased a maximum of 7-fold in the WKY and 4.5-fold in the SHR kidney from its lowest rate at

3 weeks of age to its maximal level of formation (Fig. 5B). As with 20-HETE, there was a trend toward increased 19-HETE formation in the SHR kidneys compared with their normotensive controls at most ages. These differences reached statistical significance between 3 and 9 weeks of age (1.3–2.0-fold increases).

Renal lauric acid metabolism. Further characterization of CYP4A enzyme activity involved the use of lauric acid, a prototypical substrate with high rates of metabolism and a simple metabolic profile. All incubations were carried out under linear conditions with respect to reaction time and protein concentration. Because it is a saturated fatty acid, lauric acid gives only the ω- and ω-1-hydroxylation products with the short incubation period used in this study. The developmental pattern of lauric acid ω- and ω-1-hydroxylase activity in WKY and SHR kidneys (Fig. 6) was similar to that observed with arachidonic acid (Fig. 5). At any given age, the lauric acid ω-hydroxylase activity was 20–30-fold higher than the corresponding arachidonic acid ω-hydroxylase activity. In the SHR kidney, the formation of 12-hydroxylauric acid was 200–900 pmol/min/mg of protein, whereas 20-HETE formation was 7.7–36 pmol/min/mg of protein.

Total cytochrome P450-dependent lauric acid metabolism increased 3–4-fold in SHR and WKY kidneys, from the lowest level at 3 weeks of age to a maximum at ~9 weeks of age. The formation of 12-hydroxylauric acid increased 4–5-fold between 3 and 5 weeks of age and remained fairly constant at 7–13 weeks (Fig. 6A). Lauric acid ω-hydroxylase activity was 25–41% higher in the 3–6-week-old SHR kidneys relative to their normotensive controls, an increase that was slightly less than the increase in arachidonic acid ω-hydroxylase activity in these samples. In older rats, there were no significant differences in renal lauric acid ω-hydroxylation between the WKY rats and SHR. The ratio of 12-hydroxylauric acid to 11-hydroxylauric acid formation was ~1.5 in 3- and 4-week-old rats and gradually increased to 2–2.6 in rats ≥9 weeks old. There were no significant differences in this ratio between the WKY rats and SHR at any age. Lauric acid ω-1-hydroxylase activity increased 3.5-fold between 3 and 5 weeks of age and remained fairly constant from 7 to 13 weeks of age (Fig. 6B). In most age groups, there was a trend toward increased 11-hydroxylauric acid formation in the SHR kidney relative to the WKY rat kidney, but this difference was significant only in the 3-week-old animals (117 ± 10 versus 144 ± 17 pmol/min/mg of protein).

CYP4A protein levels. Western blots were used to compare the CYP4A immunoreactive protein levels in the WKY and SHR kidneys (Fig. 7). The antibody was made against clofibrate-induced rat liver CYP4A1 and reportedly cross-reacts with CYP4A2 and CYP4A3. Two CYP4A immunoreactive proteins were detected in all samples, and the developmental pattern of expression was consistent with the pattern of CYP4A mRNA (Fig. 2) and enzyme activity (Figs. 5A and 6A). Interestingly, the slower mobility protein in the 1–4-week-old samples shifts to a higher apparent mass in the older samples. In some 5-week-old samples, all three protein bands could be detected. Strain- and tissue-dependent patterns of reactivity were apparent with this antibody and prevented the assignment of protein bands to the individual CYP4A isoforms. Consistent with differences in CYP4A mRNA and activity measurements, CYP4A protein levels were increased 2–3-fold in 1–5-week-old SHR kidneys relative to age-matched WKY rat kidneys. In the older animals, there were no differences between the amount of CYP4A immunoreactive protein in the SHR and WKY rat kidneys, which is consistent with the lack of significant differences in enzyme activity and CYP4A mRNA levels. The dramatic increase in CYP4A protein levels after 4 weeks of age likely reflects the increased CYP4A2 expression at this time.

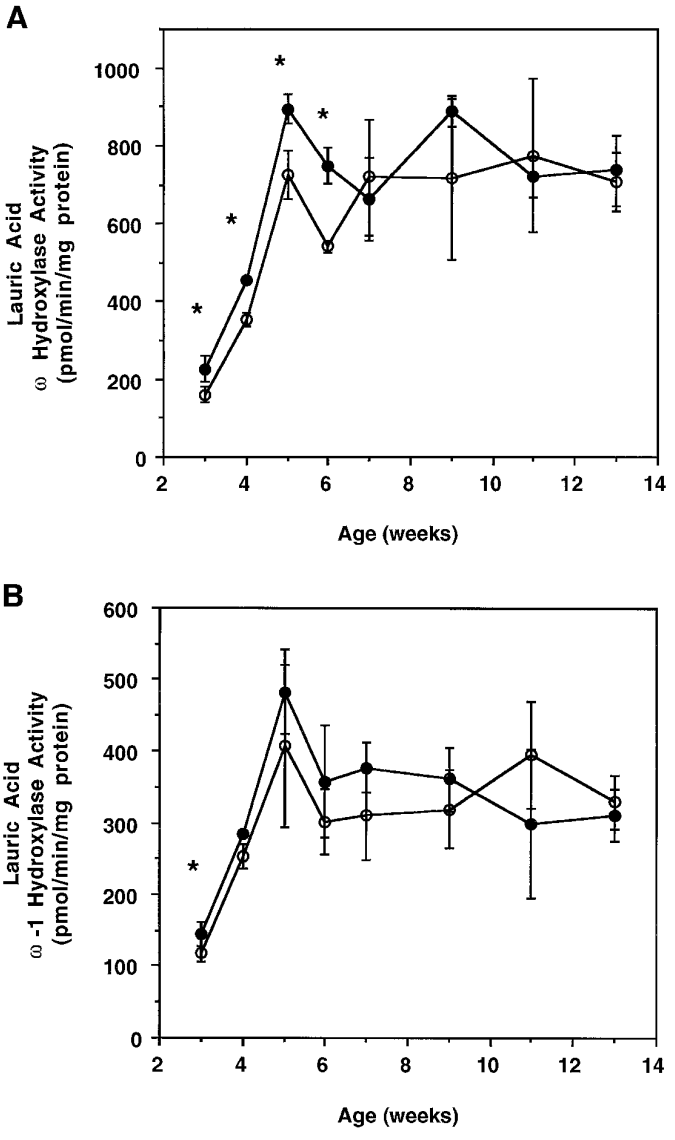

Fig. 6. Renal lauric acid ω- and ω-1-hydroxylase activity throughout development in the WKY rat and SHR. Lauric acid ω (A) and ω-1 (B)-hydroxylase activity was measured as the NADPH-dependent formation of 12-hydroxylauric acid and 11-hydroxylauric acid, respectively, in incubations of WKY rat (○) and SHR (●) renal microsomes with [^{14}C]lauric acid. Values are mean ± standard deviation from three to six animals of a given age and strain. Significant differences between WKY rat and SHR kidneys at a given age are indicated ($p < 0.05$). Lauric acid ω-hydroxylase activity reflects CYP4A enzyme activity, whereas hydroxylation at the ω-1 position is also dependent on CYP2C and CYP2E1 activity.

Discussion

Differences in arachidonic acid ω-hydroxylase activity in renal microsomes from SHR and WKY rats have been recognized for several years (13, 15, 16, 24); however, detailed

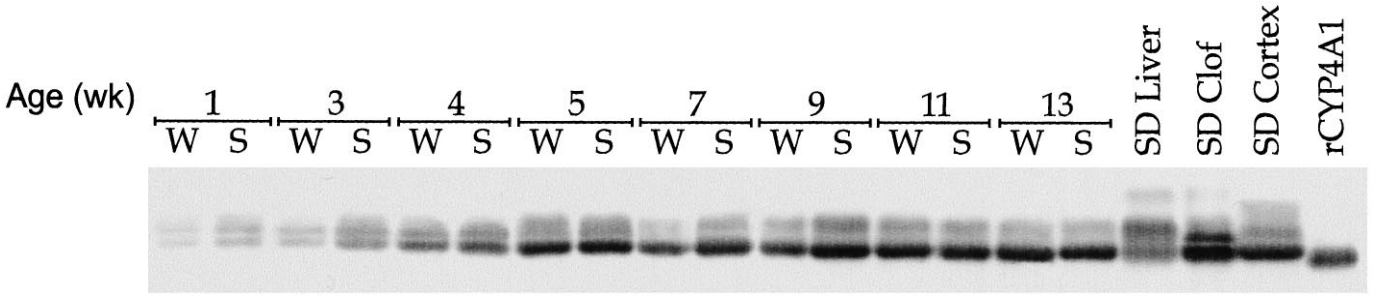

Fig. 7. Western immunoblot of CYP4A proteins in the WKY rat and SHR kidneys. Renal microsomes from WKY rat (*W*) and SHR (*S*) were separated on a 8% SDS-polyacrylamide gel, transferred to nitrocellulose, and blotted with goat anti-CYP4A1 antisera. Immunoreactive proteins were detected by alkaline phosphatase staining. The blot is representative of the expression of CYP4A proteins in samples from three to six animals of a given age and strain. Liver, clofibrate (*Clof*)-induced liver, and cortical (*Cortex*) microsomes prepared from Sprague-Dawley rats and purified CYP4A1 expressed in *Escherichia coli* (rCYP4A1) were included as controls. Two immunoreactive proteins were detected in all microsomal samples, and the lower mobility protein shifts to a higher apparent mass in the older samples.

studies of the contribution of the individual CYP genes to these differences are lacking. This report is the first characterization of specific *CYP4A* gene expression throughout development in the WKY rat and SHR kidney. These studies suggest that the *CYP4A* genes are not consistently expressed at higher levels in the SHR kidney relative to the WKY rat kidney. Although the levels of CYP4A3 and CYP4A8 mRNA and CYP4A immunoreactive protein were significantly increased in the kidneys of prehypertensive SHR rats, these differences disappeared after 4 weeks of age. The changes in CYP4A mRNA and protein levels were accompanied by parallel changes in CYP4A enzyme activity measured as arachidonic acid or lauric acid ω-hydroxylation. The increased expression of CYP4A at both the mRNA and protein level in the 1–4-week-old SHR is also consistent with the increase in arachidonic acid ω-hydroxylation in young SHR previously reported (13, 15, 16). The current results suggest that the increased CYP4A protein and activity levels in these young SHR are due to increased expression of CYP4A3 and/or CYP4A8 during this period. The increased expression of these genes in the 1–4-week-old animals is of interest for several reasons. First, CYP4A3 is the major CYP4A isoform expressed before 4 weeks of age and therefore is likely to play a significant role in renal 20-HETE formation during this period. Maximal differences in 20-HETE formation between SHR and WKY rat kidneys during this time are consistent with a major role for CYP4A3 in the generation of this eicosanoid in the immature rat kidney. In addition, critical changes in renal blood flow and resetting of the pressure-natriuresis relationship have been described in the kidneys of prehypertensive SHR (<5 weeks of age) and may be necessary for the development of hypertension in this experimental model (10). One proposed mediator of these renal function changes in the young SHR is the potent vasoconstrictor 20-HETE (10, 15). The current observation of increased CYP4A3 and CYP4A8 expression in the prehypertensive SHR kidney suggests that the regulation of these genes during this critical period of development may have a significant impact on renal function and the maintenance of the pressure-natriuresis relationship and therefore blood pressure.

In the SHR, blood pressure is significantly increased relative to the WKY rat from 5 weeks of age and remains elevated thereafter (31). Alterations in CYP4A expression do not accompany the increased blood pressure; CYP4A mRNA and protein levels were generally comparable between the hypertensive and normotensive rat kidneys after 4 weeks of age. A trend toward increased CYP4A enzyme activity in the SHR kidney was detectable through 9 weeks of age. However, beyond 5 weeks of age, 20-HETE formation was only 1.2–1.4-fold higher in the SHR than in the WKY rat and thus significantly less than the 1.7–2-fold increases detected in the prehypertensive SHR kidneys. This is consistent with Omata *et al*. (13), who found the largest increase in 20-HETE formation between 1 and 3 weeks of age (2–3-fold) and only 1.3–1.5-fold increases in older animals.

To confirm the pattern of CYP4A enzyme activity in WKY rat and SHR kidneys parallel comparisons were made with a second substrate for the CYP4A enzymes, lauric acid. Measurement of arachidonic acid ω-hydroxylase activity has previously been complicated by the subsequent metabolism of 20-HETE to the dicarboxylic acid metabolite, 20-carboxyarachidonic acid (13). Lauric acid was therefore selected to avoid subsequent metabolism and to give a much simpler measure of CYP4A activity. Although it is reasonable to hypothesize that the individual rat CYP4A isoforms may have unique substrate specificities, similar to that described for the multiple rabbit CYP4A isoforms (32, 33), there were no apparent differences in metabolism between these two substrates with WKY rat and SHR renal microsomes. Lauric acid ω-hydroxylation activity was consistent with arachidonic acid ω-hydroxylation, although the magnitude of the differences in activity between WKY rat and SHR kidneys was smaller with lauric acid. In fact, no differences in lauric acid ω-hydroxylation between SHR and WKY animals were apparent beyond 6 weeks of age, which is consistent with the comparable levels of CYP4A mRNA and protein at these times. In contrast, Imaoka and Funae (24) reported a 68% increase in lauric acid ω-hydroxylase activity and a 113% increase in lauric acid ω-1-hydroxylase activity in renal microsomes from 12-week-old SHR relative to WKY animals, which they attributed to the 1.4-fold higher levels of renal CYP4A2 protein in the SHR kidneys. Similar differences were not apparent in the current study nor are they consistent with the lack of differences in 20-HETE formation between older WKY rats and SHR reported in several other studies (12, 13).

The RNase protection assay developed for these studies is much more specific and sensitive than previous methods for detecting expression of the CYP4A mRNAs. With this assay,

CYP4A3 expression could be quantified in 1-week-old kidneys, whereas both CYP4A1 and CYP4A8 were detectable by 3 weeks of age. Expression of both CYP4A1 and CYP4A3 decreased dramatically after 5 weeks of age to as low as 20% of their maximal expression levels, and their mRNAs were still easily detected. This is in contrast to several previous reports describing little or no basal expression of CYP4A1 and CYP4A3 in the kidneys of immature and mature rats as measured by Northern blot analysis with gene-specific oligonucleotide probes (22, 34–36). Although these studies used Sprague-Dawley or Fisher 344 strains, work in our laboratory has indicated that the pattern of expression of the renal *CYP4A* genes in Sprague-Dawley rats is indistinguishable from that found in the WKY rat and SHR kidney. The expression of renal CYP4A2 has previously been shown to be specific for males, regulated in part by thyroid hormone and testosterone, and to be undetectable in the kidneys of immature rats (34, 36). In the current study, we did not detect basal CYP4A2 expression in male rat kidneys younger than 5 weeks of age by RNase protection assay. However, using a gene-specific RT-PCR approach, we were able to detect CYP4A2 mRNA as early as 1 week of age. The fact that CYP4A2 expression in the 1–4-week-old rat kidney is so low that it is detectable only by RT-PCR is not consistent with the report by Iwai and Inagami (25) of a 4-fold increase in CYP4A2 mRNA in the 10-day- and 4-week-old SHR rat kidney relative to the age-matched WKY rat kidney. Because the Northern blot analysis in that study used a full-length CYP4A2 cDNA probe, which would significantly cross-hybridize with CYP4A3 (97% nucleotide identity) and possibly CYP4A1 and CYP4A8 (66% and 72% identical, respectively), it is likely that the increased CYP4A2 expression in the 10-day- and 4-week-old SHR kidneys reported by Iwai and Inagami reflects changes in CYP4A3 mRNA levels.

A number of issues with regard to the significance of the CYP4A enzymes in the regulation of renal function and blood pressure remain unanswered. A clear role has been established for 20-HETE in the regulation of renal vascular tone and ion transport (2, 3, 5); however, the multiplicity and complex regulatory pattern of the *CYP4A* gene family within the kidney make it difficult to discern the importance of the individual CYP4A isoforms in the generation of 20-HETE. Detailed studies with the individual CYP4A proteins expressed *in vitro* are necessary to fully understand the importance of each of these proteins in eicosanoid formation. Based on information from other species, it is likely that kinetic differences in fatty acid metabolism as well as distinct patterns of fatty acid selectivity will be revealed from such studies. In the current study, significant differences in CYP4A expression between SHR and WKY rat kidneys were detected only during the prehypertensive stage of development; however, this does not preclude the existence of physiologically significant differences that are localized to specific structures within the nephron. Gross dissection of the kidney indicates that CYP4A expression is similar in the cortex and outer medulla, but these regions comprise of a number of diverse structures. Arachidonic acid ω-hydroxylase activity has been localized to the proximal tubules, whereas ω-1-hydroxylation is more widespread throughout the nephron (14). The detection of arachidonic acid ω-hydroxylase activity within the renal vasculature itself also suggests that CYP4A expression is localized to areas in which the ensuing eicosanoid formation is of physiological significance (37). Schwartzman *et al*. (38) reported the localization of CYP4A immunoreactive protein and CYP4A mRNA to the S2 and S3 fragments of the proximal tubule with much lower levels in the cortical collecting, distal convoluted, and connecting tubules. However, the lack of specific probes did not permit identification of the specific CYP4A isoforms that were expressed in these regions (38). The RNase protection assays developed for this study provide a valuable tool to localize the expression of the *CYP4A* genes to more discrete regions of the nephron. A detailed pattern of CYP4A expression along the nephron, coupled with a kinetic characterization of fatty acid oxidation by each of the CYP4A proteins, may provide some clues as to why multiple enzymes exist for an apparently limited repertoire of catalytic function. The age-dependent pattern of expression of the *CYP4A* genes raises important questions regarding their role in renal function and blood pressure. The fact that CYP4A expression was elevated in the prehypertensive stage of development in the SHR supports a role for these genes in the initial changes in renal function during this period. Maximal levels of expression of the CYP4A1 and CYP4A3 genes in the immature rat kidney are also consistent with a role in nephrogenesis. 20-HETE is known to be mitogenic in rat proximal tubule cells and is a proposed mediator of the effect of epidermal growth factor on cell growth (39). A role for prostaglandin metabolites of arachidonic acid in postnatal nephrogenesis was recently described in mice lacking the cyclooxygenase-2 gene (40), and it is possible that cytochrome P450 metabolites have similar functions. Finally, the cellular signaling mechanisms through which the CYP4A-mediated eicosanoids exert their varied effects is also of interest and may reveal potential targets for modulation of renal eicosanoid formation.

Acknowledgments

We thank Frank J. Gonzalez (National Cancer Institute, Bethesda, MD) for providing the CYP4A1 and CYP4A3 plasmids, Bill Howald and the mass spectrometry facility of the University of Washington School of Pharmacy for GC-MS analysis, Philip Yook and Milena Sadee for technical assistance, and Jeffrey A. Silverman for helpful discussions and thoughtful review of the manuscript.

References

1. Nelson, D. R., L. Koymans, T. Kamataki, J. J. Stegeman, R. Feyereisen, D. J. Waxman, M. R. Waterman, O. Gotoh, M. J. Coon, R. W. Estabrook, I. C. Gunsalus, and D. W. Nebert. P450 superfamily: update on new sequences, gene mapping, accession numbers and nomenclature. *Pharmacogenetics* **6:**1–42 (1996).
2. Escalante, B., D. Erlij, J. R. Falck, and J. C. McGiff. Effect of cytochrome P450 arachidonate metabolites on ion transport in rabbit kidney loop of Henle. *Science (Washington D. C.)* **251:**799–802 (1991).
3. Wang, W., and M. Lu. Effect of arachidonic acid on activity of the apical K^+ channel in the thick ascending limb of the rat kidney. *J. Gen. Physiol.* **106:**727–743 (1995).
4. Zou, A. P., J. D. Imig, P. R. Ortiz de Montellano, Z. Sui, J. R. Falck, and R. J. Roman. Effect of P-450 ω-hydroxylase metabolites of arachidonic acid on tubuloglomerular feedback. *Am. J. Physiol.* **266:**F934–F941 (1994).
5. Ma, Y. H., D. Gebremedhin, M. L. Schwartzman, J. R. Falck, J. E. Clark, B. S. Masters, D. R. Harder, and R. J. Roman. 20-Hydroxyeicosatetraenoic acid is an endogenous vasoconstrictor of canine renal arcuate arteries. *Circ. Res.* **72:**126–136 (1993).
6. Escalante, B., J. R. Falck, P. Yadagiri, L. M. Sun, and M. Laniado-Schwartzman. 19(S)-Hydroxyeicosatetraenoic acid is a potent stimulator of renal Na^+-K^+-ATPase. *Biochem. Biophys. Res. Commun.* **152:**1269–1274 (1988).
7. Carroll, M. A., M. Balazy, P. Margiotta, J. R. Falck, and J. C. McGiff. Renal vasodilator activity of 5,6-epoxyeicosatrienoic acid depends upon conversion by cyclooxygenase and release of prostaglandins. *J. Biol. Chem.* **268:** 12260–12266 (1993).

8. Satoh, T., H. T. Cohen, and A. I. Katz. Intracellular signaling in the regulation of renal Na-K-ATPase. II. Role of eicosanoids. *J. Clin. Invest.* **91:**409–415 (1993).
9. Bianchi, G., U. Fox, G. F. Di Francesco, A. M. Giovanetti, and D. Pagetti. Blood pressure changes produced by kidney cross-transplantation between spontaneously hypertensive rats and normotensive rats. *Clin. Sci. Mol. Med.* **47:**435–448 (1974).
10. Cowley, A. W., Jr., and R. J. Roman. The role of the kidney in hypertension. *JAMA* **275:**1581–1589 (1996).
11. Sacerdoti, D., B. Escalante, N. G. Abraham, J. C. McGiff, R. D. Levere, and M. L. Schwartzman. Treatment with tin prevents the development of hypertension in spontaneously hypertensive rats. *Science (Washington D. C.)* **243:**388–390 (1989).
12. Gebremedhin, D., Y. H. Ma, J. D. Imig, D. R. Harder, and R. J. Roman. Role of cytochrome P-450 in elevating renal vascular tone in spontaneously hypertensive rats. *J. Vasc. Res.* **30:**53–60 (1993).
13. Omata, K., N. G. Abraham, B. Escalante, and M. L. Schwartzman. Age-related changes in renal cytochrome P-450 arachidonic acid metabolism in spontaneously hypertensive rats. *Am. J. Physiol.* **262:**F8–F16 (1992).
14. Omata, K., N. G. Abraham, and M. L. Schwartzman. Renal cytochrome P-450-arachidonic acid metabolism: localization and hormonal regulation in SHR. *Am. J. Physiol.* **262:**F591–F599 (1992).
15. Imig, J. D., J. R. Falck, D. Gebremedhin, D. R. Harder, and R. J. Roman. Elevated renovascular tone in young spontaneously hypertensive rats: role of cytochrome P-450. *Hypertension (Dallas)* **22:**357–364 (1993).
16. Stec, D. E., M. R. Trolliet, J. E. Krieger, H. J. Jacob, and R. J. Roman. Renal cytochrome P4504A activity and salt sensitivity in spontaneously hypertensive rats. *Hypertension (Dallas)* **27:**1329–1336 (1996).
17. Schwartzman, M. L., K. Omata, F. M. Lin, R. K. Bhatt, J. R. Falck, and N. G. Abraham. Detection of 20-hydroxyeicosatetraenoic acid in rat urine. *Biochem. Biophys. Res. Commun.* **180:**445–459 (1991).
18. Aoyama, T., J. P. Hardwick, S. Imaoka, Y. Funae, H. V. Gelboin, and F. J. Gonzalez. Clofibrate-inducible rat hepatic P450s IVA1 and IVA3 catalyze the ω- and (ω-1)-hydroxylation of fatty acids and the ω-hydroxylation of prostaglandins E1 and F2 *alpha*. *J. Lipid Res.* **31:**1477–1482 (1990).
19. Imaoka, S., S. Tanaka, and Y. Funae. ω- and (ω-1)-hydroxylation of lauric acid and arachidonic acid by rat renal cytochrome P-450. *Biochem. Int.* **18:**731–740 (1989).
20. Laethem, R. M., M. Balazy, J. R. Falck, C. L. Laethem, and D. R. Koop. Formation of 19(S)-, 19(R)-, and 18(R)-hydroxyeicosatetraenoic acids by alcohol-inducible cytochrome P450 2E1. *J. Biol. Chem.* **268:**12912–12918 (1993).
21. Laethem, R. M., and D. R. Koop. Identification of rabbit cytochromes P450 2C1 and 2C2 as arachidonic acid epoxygenases. *Mol. Pharmacol.* **42:**958–963 (1992).
22. Kimura, S., J. P. Hardwick, C. A. Kozak, and F. J. Gonzalez. The rat clofibrate-inducible CYP4A subfamily. II. cDNA sequence of IVA3, mapping of the Cyp4a locus to mouse chromosome 4, and coordinate and tissue-specific regulation of the CYP4A genes. *DNA* **8:**517–525 (1989).
23. Stromstedt, M., S. Hayashi, P. G. Zaphiropoulos, and J. A. Gustafsson. Cloning and characterization of a novel member of the cytochrome P450 subfamily IVA in rat prostate. *DNA Cell Biol.* **9:**569–577 (1990).
24. Imaoka, S., and Y. Funae. Hepatic and renal cytochrome P-450s in spontaneously hypertensive rats. *Biochim. Biophys. Acta* **1074:**209–213 (1991).
25. Iwai, N., and T. Inagami. Isolation of preferentially expressed genes in the kidneys of hypertensive rats. *Hypertension (Dallas)* **17:**161–169 (1991).
26. Frederick, R. B., M. Ausbel, R. E. Kingston, D. D. Moore, J. G. Seidman, J. A. Smith, and K. Struhl, eds. *Current Protocols in Molecular Biology*. John Wiley & Sons, New York (1994).
27. Hod, Y. A simplified ribonuclease protection assay. *Biotechniques* **13:**852–854 (1992).
28. Okita, R. T., J. E. Clark, J. R. Okita, and B. S. Masters. ω- and (ω-1)-hydroxylation of eicosanoids and fatty acids by high-performance liquid chromatography. *Methods Enzymol.* **206:**432–441 (1991).
29. Oliw, E. H., J. A. Lawson, A. R. Brash, and J. A. Oates. Arachidonic acid metabolism in rabbit renal cortex: formation of two novel dihydroxyeicosatrienoic acids. *J. Biol. Chem.* **256:**9924–9931 (1981).
30. Oliw, E. H., and P. Moldeus. Metabolism of arachidonic acid by isolated rat hepatocytes, renal cells and by some rabbit tissues: detection of vicinal diols by mass fragmentography. *Biochim. Biophys. Acta* **721:**135–143 (1982).
31. Beierwaltes, W. H., W. J. Arendshorst, and P. J. Klemmer. Electrolyte and water balance in young spontaneously hypertensive rats. *Hypertension (Dallas)* **4:**908–915 (1982).
32. Roman, L. J., C. N. Palmer, J. E. Clark, A. S. Muerhoff, K. J. Griffin, E. F. Johnson, and B. S. Masters. Expression of rabbit cytochromes P4504A which catalyze the ω-hydroxylation of arachidonic acid, fatty acids, and prostaglandins. *Arch. Biochem. Biophys.* **307:**57–65 (1993).
33. Johnson, E. F., D. L. Walker, K. J. Griffin, J. E. Clark, R. T. Okita, A. S. Muerhoff, and B. S. Masters. Cloning and expression of three rabbit kidney cDNAs encoding lauric acid ω-hydroxylases. *Biochemistry* **29:**873–879 (1990).
34. Sundseth, S. S., and D. J. Waxman. Sex-dependent expression and clofibrate inducibility of cytochrome P450 4A fatty acid ω-hydroxylases: male specificity of liver and kidney CYP4A2 mRNA and tissue-specific regulation by growth hormone and testosterone. *J. Biol. Chem.* **267:**3915–3921 (1992).
35. Prough, R. A., S. J. Webb, H. Q. Wu, D. P. Lapenson, and D. J. Waxman. Induction of microsomal and peroxisomal enzymes by dehydroepiandrosterone and its reduced metabolite in rats. *Cancer Res.* **54:**2878–2886 (1994).
36. Webb, S. J., G. H. Xiao, T. E. Geoghegan, and R. A. Prough. Regulation of CYP4A expression in rat by dehydroepiandrosterone and thyroid hormone. *Mol. Pharmacol.* **49:**276–287 (1996).
37. Kauser, K., J. E. Clark, B. S. Masters, P. R. Ortiz de Montellano, Y. H. Ma, D. R. Harder, and R. J. Roman. Inhibitors of cytochrome P-450 attenuate the myogenic response of dog renal arcuate arteries. *Circ. Res.* **68:**1154–1163 (1991).
38. Schwartzman, M. L., J. L. da Silva, F. Lin, M. Nishimura, and N. G. Abraham. Cytochrome P450 4A expression and arachidonic acid ω-hydroxylation in the kidney of the spontaneously hypertensive rat. *Nephron* **73:**652–663 (1996).
39. Lin, F., A. Rios, J. R. Falck, Y. Belosludtsev, and M. L. Schwartzman. 20-Hydroxyeicosatetraenoic acid is formed in response to EGF and is a mitogen in rat proximal tubule. *Am. J. Physiol.* **269:**F806–F816 (1995).
40. Morham, S. G., R. Langenbach, C. D. Loftin, H. F. Tiano, N. Vouloumanos, J. C. Jennette, J. F. Mahler, K. D. Kluckman, A. Ledford, C. A. Lee, and O. Smithies. Prostaglandin synthase 2 gene disruption causes severe renal pathology in the mouse. *Cell* **83:**473–482 (1995).

Send reprint requests to: Deanna L. Kroetz, Ph.D., Department of Biopharmaceutical Sciences, University of California, San Francisco, 513 Parnassus, Box 0446, San Francisco, CA 94143-0446. E-mail: deanna@itsa.ucsf.edu